

FABRICATION AND TESTING OF VERTICALLY-ACTUATED POLYCRYSTALLINE SiC MICROMECHANICAL RESONATORS FOR MHZ FREQUENCY APPLICATIONS

Robert F. Wiser, Christian A. Zorman, and Mehran Mehregany
 Department of Electrical Engineering and Computer Science
 Case Western Reserve University, Cleveland, Ohio 44106

ABSTRACT

Vertically-actuated micromechanical resonators operating at MHz frequencies were fabricated from phosphorus-doped polycrystalline silicon carbide (poly-SiC) films. The films were deposited on thin polysilicon sacrificial layers by atmospheric pressure chemical vapor deposition (APCVD) and surface micromachined into structures using a lift-off patterning technique. The resonators were tested under high vacuum conditions using a transimpedance amplifier-based circuit. The measured resonant frequencies were consistent with what was expected based on device designs and material properties; however, the quality factors were much lower than expected. Equivalent circuit modeling suggested that the low quality factors were due to the electrical resistance of the beams, which was unexpectedly high.

INTRODUCTION

To expand the use of micromechanical resonators well into the UHF range, alternatives to polysilicon, namely silicon carbide (SiC) [1] and diamond [2] are currently being developed. These materials are attractive for such applications because they possess higher acoustic velocities (i.e., $(E/\rho)^{1/2}$) relative to polysilicon, which translates to higher resonant frequencies for the same geometry. Surface micromachining processes have been developed for both materials, with SiC currently at the forefront due to more mature processing technologies that in most instances are quite similar to silicon.

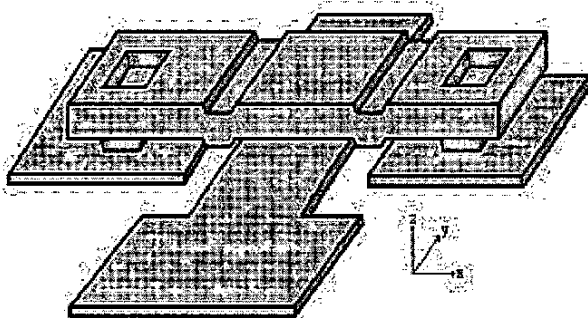


Figure 1 Schematic diagram of a vertically-actuated resonator with a poly-SiC drive electrode and C-C beam.

The purpose of this study was to fabricate and test polycrystalline SiC (poly-SiC) clamped-clamped (C-C) beam micromechanical resonators designed for MHz frequency applications. The C-C beam resonators, shown schematically in Fig. 1, incorporated drive electrodes and beams made from poly-SiC and were based on designs

that were successfully implemented with polysilicon as the structural layer. Fabrication of these devices out of poly-SiC poses several significant challenges in the areas of film growth and patterning. These challenges stem mainly from the fact that the poly-SiC resonating bridge is suspended over an anchored poly-SiC electrode with an air gap that is defined by a sub-micron thick sacrificial layer. For polysilicon, use of such thin sacrificial layers is routine; however, issues related to the high temperatures used to deposit poly-SiC and the methods available to pattern the as-deposited, films pose significant impediments to the successful fabrication of such devices.

FABRICATION DETAILS

The C-C beam process flow is shown schematically in Fig. 2(a)-(d). The fabrication process began with a 4-inch, p-type Si wafer on which a 2 μm -thick SiO_2 film was grown by wet thermal oxidation. The wafer was then coated with a 2000 \AA -thick Si_3N_4 film to protect the oxide from the subsequent processing steps and to provide additional electrical isolation. Because reactive ion etching (RIE) of SiC generally suffers from poor selectivity to silicon-derivative materials, especially polysilicon, the poly-SiC electrodes and beams were patterned using a lift-off patterning process first reported elsewhere [3]. A lift-off mold for the poly-SiC electrode was fabricated from a 1.5 μm -thick, low-temperature oxide (LTO) that was photolithographically defined and etched using a two step procedure, with about 1.2 μm removed by RIE followed by a buffered oxide etch (BOE) to remove the remaining LTO. A 1000 \AA -thick phosphorus-doped, poly-SiC film was then deposited by APCVD using a single-step recipe performed at 1280 $^\circ\text{C}$. In this recipe, C_3H_8 and SiH_4 are used as source gases, H_2 as a carrier gas and PH_3 as a dopant gas [4]. As expected, the poly-SiC film was deposited over the entire wafer, but the conformality over the steps of the molds was poor and the film had poor adhesion to the top of the mold. Lift-off was achieved by first immersing the wafer in BOE for 20 min, then at various times, immersing it in a DI water bath with ultrasonic agitation for 15-30s. Large areas of poly-SiC film could then be removed by hand-polishing the wafer. This procedure was repeated until the poly-SiC was removed from the field areas.

Next an undoped, 3000 \AA -thick polysilicon sacrificial layer was deposited using LPCVD. Photolithography was used to define an etch mask for anchor windows and a chlorine-based RIE was used to remove the polysilicon sacrificial layer in the anchor regions. A 3 μm -thick LTO layer was then deposited by LPCVD. The LTO film was photolithographically patterned to define the mold for the beam. About 2.9 μm of LTO was etched using a timed RIE,

with the remaining LTO etched by a timed BOE. A 3:1 liftoff mold-to-poly-SiC thickness ratio was used to facilitate the liftoff process.

A 1 μm -thick poly-SiC beam layer was then deposited using a two-step carbonization-based APCVD recipe originally designed for epitaxial growth of 3C-SiC on Si wafers [5]. The carbonization-based recipe was essentially the same as the single step recipe except that the surface of the polysilicon was converted to poly-SiC by exposing it to C_3H_8 at 1280°C prior to film growth. The carbonization-based recipe produces higher quality poly-SiC films on polysilicon surfaces than the single step recipes [4], and thus was used here. After the second poly-SiC deposition, the unwanted film in the field area was removed using the liftoff process.

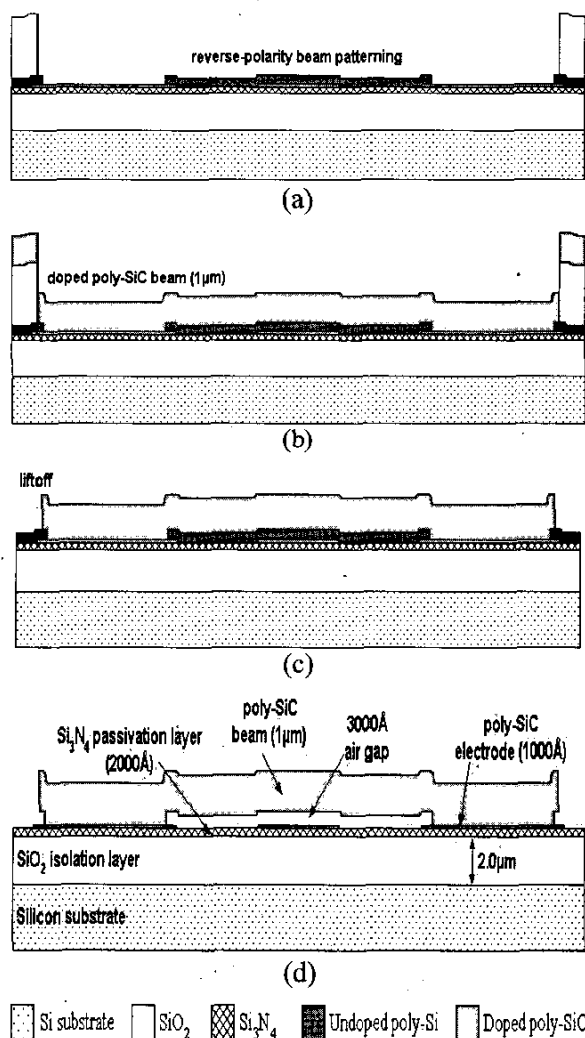


Figure 2 Cross-sectional schematics of the key lift-off based fabrication steps: (a) after patterning the lift-off mold; (b) after SiC deposition; (c) after lift-off; and (d) final device.

Devices were released by dissolving the thin polysilicon layer using an aggressive, ultrasonically agitated $\text{HF}:\text{HNO}_3:\text{H}_2\text{O}$ isotropic wet etch. Since much of the field area was composed of Si_3N_4 , a mixture of 100 mL DI H_2O , 200 mL HNO_3 , and 100 mL HF (1:2:1) was used. Complete removal of the polysilicon sacrificial layer for about 85% of the devices was accomplished in 10 min, with the remaining devices requiring an additional 2 min. The release was followed by a 15 min rinse in DI water and a hot-plate assisted air-dry step. Supercritical drying was not necessary for any of the devices in this study despite the 3000Å-thick sacrificial gaps. Since the sacrificial gap spacing was so small, proper release was determined by checking the resistivity between the drive electrode and the sense pad connected to the beam, with an open circuit reading indicating a fully released beam. Fig. 3 is a SEM micrograph of a typical micromechanical resonator showing both the C-C beam and the underlying electrode. For this study, the 1 μm -thick beams ranged in length from 51 to 110 μm .

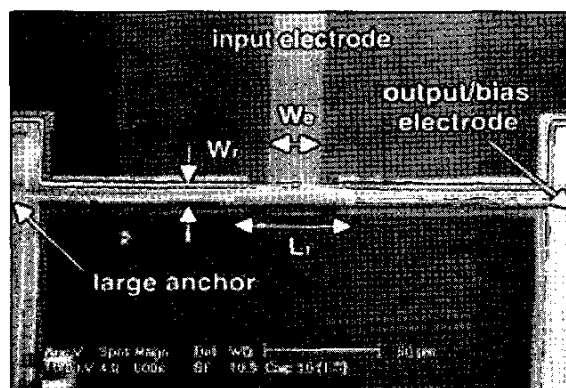


Figure 3. SEM micrograph of a poly-SiC resonator. The beam length (L_r), beam width (W_r), and electrode width (W_e), as well as input and output electrodes are shown.

DEVICE TESTING AND DATA ANALYSIS

Electrical measurements were made using a motional current and amplification scheme developed by others and described in detail elsewhere [6]. After dicing each wafer, chips were mounted to printed circuit boards that contained the components required for the electrical measurement and based around a Phillips SA5211 transimpedance amplifier as shown in Fig. 4. For each resonator, the beam was used as the bias and sense electrode while the fixed electrode was used to drive the beam into resonance. An Agilent 4395A network analyzer was used to provide the frequency-swept sinusoidal input excitation voltage to the device and to sense the output voltage of the amplifier. The network analyzer was set to record the power of the input signal compared to the reference signal as a function of frequency. A dc bias (0 to 30 V) could be applied to the capacitive gap to induce a motional current in the beam via an HP6209B power supply.

All resonator testing was performed in a custom-built vacuum chamber capable of reaching pressures below 10

μ Torr. To connect the PCB to the external components, shielded electrical feedthroughs were used to pass the drive and sense signals, and unshielded wire feedthroughs were used to provide the ground and dc biasing paths. The vacuum chamber utilized a turbomolecular and roughing pump combination capable of reaching base pressures in the 10^{-6} Torr range. Testing was always performed below 1×10^{-3} Torr to negate the effects of squeeze-film damping. For determination of Q , testing was performed at pressures around 1.5×10^{-5} Torr.

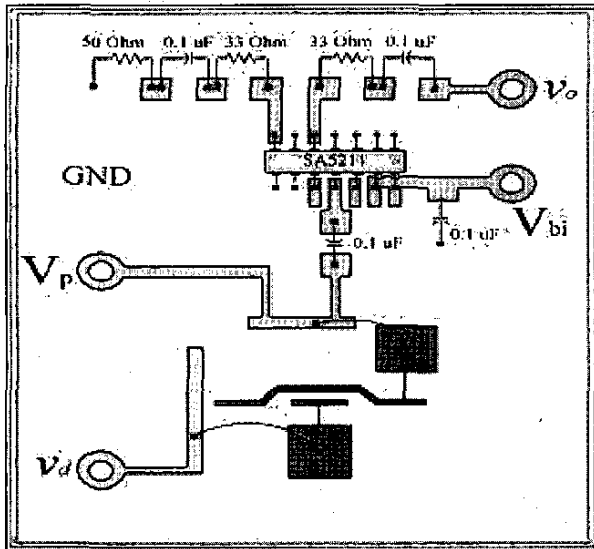


Figure 4 PCB circuit used for vacuum testing of the poly-SiC C-C beam resonators.

Table 1 is a summary of the resonant frequencies and device dimensions for the three main resonator designs evaluated in this project. The average resonant frequency ranged from 1.5 MHz for the 110 μ m-long beams to 4.0 MHz for the 51 μ m-long beams. Variations in the dimensions were related to processing conditions. In general, the resonant frequencies were as expected assuming a value of Young's modulus for poly-SiC of 448 GPa [7].

Average Length (μ m)	Average Width (μ m)	Average Thickness (μ m)	Average Frequency (MHz)
52.3 ± 0.5	8.9 ± 0.3	0.64 ± 0.03	3.99 ± 0.1
86.2 ± 0.3	9.3 ± 0.2	0.70 ± 0.03	2.10 ± 0.2
110.8 ± 0.6	9.2 ± 0.2	0.68 ± 0.03	1.5 ± 0.1

Table 1. Resonant frequency and beam dimensions for the three designs included in this study.

Figure 5 is a typical transmission spectrum from a 110 μ m-long C-C beam. As seen in this figure, the resonant frequency of the beam can readily be

determined, but determining the Q of the structure was very difficult due to the less than -3dB drop in the spectrum. By extrapolating Q using the half-width half maximum (HWHM) of the series resonant peak as the frequency increases toward the parallel resonance dip, a value of 128 was estimated from this spectrum as the upper bound for Q for this device.

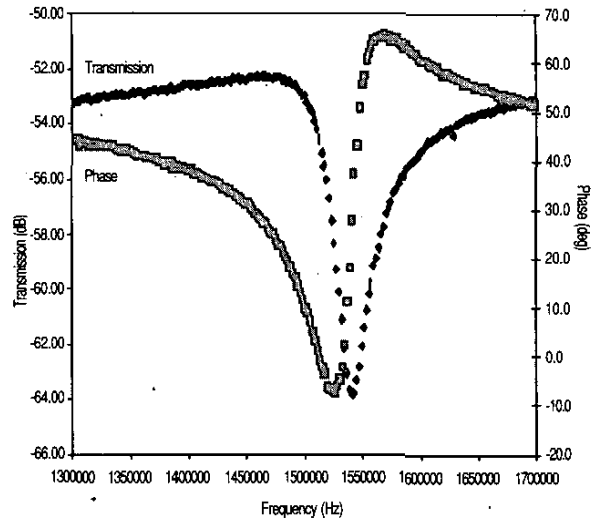


Figure 5. Frequency spectra (transmission and phase) for a 110 μ m long C-C poly-SiC beam.

To better understand the surprisingly low Q values observed for these devices, an equivalent circuit model incorporating a parasitic series resistance was created. A schematic of the circuit is shown in Fig. 6. Simulation of this circuit was performed using WinSpice™ circuit modeling software. In this circuit, a parasitic series resistance was included in series with the LCR oscillator tank, and the load was set by the transimpedance amplifier. In the simulation, the RF choke was set at 0.1 H, R_{load} at 200 Ω , C_{block} at 0.1 μ F, and the C_p at 0.15 pF. The LCR tank values were 1.08 H, 10.1 fF, and 69.8 k Ω for L_x , C_x , and R_x , respectively. Values for the parasitic series resistance ranged from 0 Ω to 5 M Ω . The simulation results in terms of frequency response, for a parasitic series resistance value of 5 M Ω is shown in Fig. 7. A comparison of this figure to the spectrum in Fig. 5 indicates that a significant parasitic series resistance is present in the testing circuit, and the effect of this resistance is to significantly reduce the value of Q . The average measured resistance of the 110 μ m-long beams was approximately 5 M Ω , indicating that the beams are, in fact, the source of this parasitic resistance. This finding is somewhat surprising given the fact that the films were *in-situ* doped with phosphorus (n-type dopant) and grown at temperatures sufficient for adequate activation.

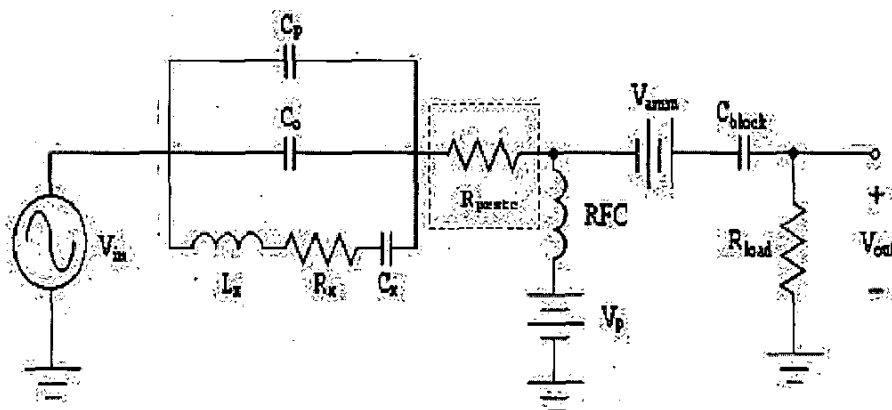


Figure 6.Equivalent circuit model accounting for a parasitic series resistance (shown in the dashed box).

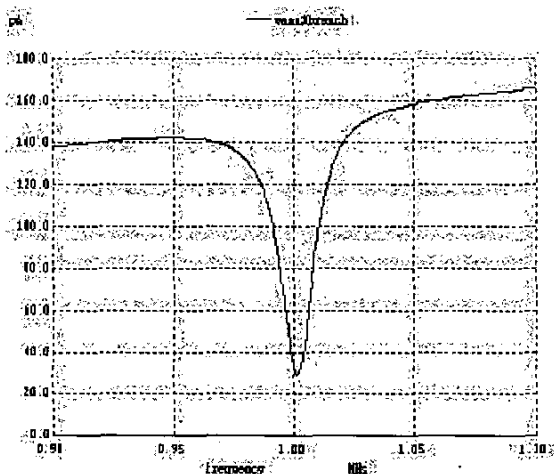


Figure 7.Simulated frequency response for the circuit in Fig. 6 with a parasitic series resistance value of 5 M Ω .

DISCUSSION AND CONCLUSIONS

The results presented here are sufficient to show that poly-SiC can be used in micromechanical devices to achieve the high resonant frequencies suggested by its Young's modulus and mass density; however, the low Q values bring to question whether it would be practical to use the material in such devices. The circuit simulation modeling suggests that inadequate doping is responsible for the low Q values and the resistance measurements substantiate this claim. However, this is not to say that low Q values are inherent to poly-SiC as a material. In fact, we have previously reported Q 's in excess of 100,000 for 2 μm -thick, poly-SiC lateral resonators designed to operate in the kHz range and made from poly-SiC films deposited in the same manner as presented in this paper [9]. These devices were not characterized electrically, but rather by scanning electron microscopy, and thus were not affected by the resistivity of the material. Furthermore, we have found that single crystal 3C-SiC lateral resonators made

using the same carbonization-based recipe presented here and characterized using the same electrical setup also have Q 's in excess of 100,000 [10]. These examples suggest that in addition to doping, geometry and microstructure may also play an important role in determining the Q of a SiC device.

ACKNOWLEDGEMENTS

The authors thank R. Jezeski for operating the silicon carbide reactor, S. Yu for wire bonding and J. Dunning for SEM. This work was supported by DARPA/MTO (Grant # DABT63-98-1-0010).

REFERENCES

- [1] X.M.H. Huang, C.A. Zorman, M. Mehregany, and M.L. Roukes, *Nature*, **421**, 496, (2003).
- [2] J. Wang, J.E. Butler, D.S.Y Hsu, and C.T.-C. Nguyen, *Proc. 2002 Sens., Act. and Microsystems Workshp.*, Hilton Head SC, June 2-6, 2002, pp. 61-62.
- [3] C.H. Wu, C.A. Zorman and M. Mehregany, *Thin Solid Films*, **355-356**, 179, (1999).
- [4] R.F. Wiser, J. Chung, M. Mehregany, and C.A. Zorman, *MRS Symp Proc.*, **741**, J4.3.1-J4.3.6, (2003).
- [5] C.A. Zorman, A.J. Fleischman, A.S. Dewa, M. Mehregany, C. Jacob, S. Nishino, and P. Pirouz, *J. Appl. Phys.*, **78**, 5136-5140, (1995).
- [6] K. Wang, A-C. Wong and C.T.-C. Nguyen, *JMEMS*, **9**, 347-360, (2000).
- [7] R.D. Carnahan, *J. Amer. Ceramic Soc.*, **51**, 223-224, (1968).
- [8] J.R. Clark, W-T. Hsu, and C.T.-C. Nyugen, *Transducers 01*, pp. 1118-1121, (2001).
- [9] S. Roy, R.G. DeAnna, C.A. Zorman, and M. Mehregany, *IEEE Trans. Elect. Dev.*, **49**, 2323-2332, (2002).
- [10] H.-I. Kuo, C.A. Zorman, and M. Mehregany, *this proceedings*.